

Adriana Zaleska*

CHARACTERISTICS OF DOPED-TiO₂ PHOTOCATALYSTS

Received June 24, 2008; reviewed; accepted July 31, 2008

Titanium dioxide represents an effective photocatalyst for water and air purification and for self-cleaning surfaces. TiO₂ shows relatively high reactivity and chemical stability under ultraviolet light ($\lambda < 387\text{nm}$), whose energy exceeds the band gap of 3.3 eV in the anatase crystalline phase. The development of photocatalysts exhibiting high reactivity under visible light ($\lambda > 380\text{nm}$) should allow the main part of the solar spectrum, even under poor illumination of interior lighting, to be used. In this work the influence of TiO₂ structure on visible light photoactivity and novel photocatalysts doped with sulfur, nitrogen, boron and carbon are presented. The photocatalytic activity of obtained powders was referred to dopant chemical form, crystalline structure, crystallite size, surface area and preparation method.

key words: doped-TiO₂, heterogeneous photocatalysis, visible light-driven photocatalysis

INTRODUCTION

Titanium dioxide has semi-conducting properties which make it an attractive material to be used as a photoactive catalyst. TiO₂ is widely used for air purification, deodorization, sterilization, anti-fouling, and mist removal (Fujishima and Zhang, 2006). Activity of TiO₂ depends on its surface area, porosity and acid-basic properties. It was also found that the photoactivity depends on the crystallite size and relative abundance of the crystallite phases (anatase/rutile). Both the crystallite size and crystalline phases modify the TiO₂ band gap. The pristine TiO₂ is only active upon ultraviolet light ($\lambda < 387\text{ nm}$) because of its band gap (3.2 eV in the anatase TiO₂ crystalline phase). To improve the photocatalytic reactivity of TiO₂ and to extend its light ab-

* Department of Chemical Technology, Gdansk University of Technology, ul. G. Narutowicza 11/12, 80-952 Gdansk, Poland, azal@chem.pg.gda.pl

sorption into the visible region, several attempts have been made: one is to dope transition metal into TiO₂ (Anpo, 2000), and another is to form reduced TiO_x photocatalysts (Takeuchi et al., 2000).

Table 1. Synthesis methods and characteristics of non-metal moped TiO₂

Doping moiety	Preparation method	Chemical composition	Photoactivity	Ref.
N	Atmospheric-pressure plasma-enhanced nanoparticles synthesis (electric discharge in mixture of N ₂ , TIP and H ₂ O, followed by calcination at 500°C)	Presence of nitrogen was confirmed by XPS technique (peaks N 1s at around 402 eV and 400 eV)	TiO _{2-x} N _x was more effective in removing of isopropanol under both UV and visible light than the un-doped TiO ₂	(Chen et al., 2007)
	Hydrolysis of TIP or TiCl ₄ with an aqueous ammonia solution, followed by calcination at 300°C, 330°C, 400°C and 500°C	TiO _{1,71} N _{0,036} (350°C) TiO _{1,85} N _{0,017} (500°C)	UV: there is no significant difference between pure and doped samples. Vis: N-TiO ₂ was active for CO photooxidation; the activity increases with increasing calcinations temperature up to 400°C and then decreases with further increase in temperature of calcination	(Sato et al., 2005)
S	Heating the TiS ₂ powder in air (sample A: at 500°C for 90 min. and sample B: at 600°C for 24h)	Sulfur presence was confirmed by XPS technique as a Ti-S bonds (signal around 160 eV)	Activity (decomposition of methylene blue) of sample A and B was comparable to that of the undoped anatase during UV irradiation. Sample A induced the photocatalytic decomposition of MB under Vis light.	(Umebayashi et al., 2003)
	Hydrolysis of TIP in ethanol in the presence of thiourea. Separation of precipitate and calcinations at temperatures from 400 to 700°C	S ⁴⁺ was substituted for some of the lattice titanium atoms. The atomic content of S on surface was 1.6%	S-TiO ₂ calcinated at 400°C for 3h showed the highest activity under visible light (λ>500 nm)	(Ohno et al., 2004)
C	Modified sol-gel process using different alkoxide precursors: Ti(OEt) ₄ ; Ti(O- <i>n</i> Pr) ₄ ; Ti(O- <i>i</i> Pr) ₄ ; Ti(O- <i>n</i> Bu) ₄ ; Ti(O- <i>i</i> Bu) ₄ ; Ti(O- <i>t</i> Bu) ₄ ; Calcination at 65°C (3 h) and 250°C(3 h)	C content [wt.%]: 0.06 Ti(OEt) ₄ ; 0.31 Ti(O- <i>n</i> Pr) ₄ 0.13 Ti(O- <i>i</i> Pr) ₄ 0.6 Ti(O- <i>n</i> Bu) ₄ 0.3 Ti(O- <i>i</i> Bu) ₄ 0.4 Ti(O- <i>t</i> Bu) ₄	4-chlorophenol conversion after 100min of irradiation by visible light: 25% for TiO ₂ obtained from Ti(OEt) ₄ ; 40% for TiO ₂ obtained from Ti(O- <i>n</i> Pr) ₄ 30% for TiO ₂ obtained from Ti(O- <i>i</i> Pr) ₄ 43% for TiO ₂ obtained from Ti(O- <i>n</i> Bu) ₄ 52% for TiO ₂ obtained from Ti(O- <i>i</i> Bu) ₄ 35% for TiO ₂ obtained from Ti(O- <i>t</i> Bu) ₄	(Lettmann et al., 2001)
B	Hydrolysis of Ti(OC ₂ H ₅) ₄ in presence of (C ₂ H ₅ O) ₃ B and 2,4-pentanedione as a organic ligand under Ar atmosphere. Calcination at 400-900°C, followed by Pt impregnation	Presence of B ₂ O ₃ was confirmed by XRD technique in sample calcinated at 400°C	Platinized B/Ti powder exhibited higher reactivity for the photocatalytic decomposition of water under UV than pure TiO ₂ loaded with Pt	(Moon et al., 2000)

* TIP - titanium tetra-isopropoxide

Both approaches introduce impurity/defect states in the band gap of TiO₂, which lead TiO₂ to absorb visible-light. However, transition metal doping, where quite local-

ized *d* states appear deep in the band gap of the host semiconductor, often results in the increase of the carrier recombination. Therefore, the lifetime of the mobile carriers may become shorter, giving lower photocatalytic activity. Reducing TiO₂ introduces localized oxygen vacancy states located at 0.75-1.18 eV below the conduction band (CBM) of TiO₂, which may promote photoreduction activity because a redox potential of the hydrogen evolution (H₂/H₂O) locates just below the CBM of TiO₂. In 2001, Asahi et al., presented a new type of visible light sensitive photocatalyst - nitrogen-doped TiO₂. Since Asahi paper, other non-metal doped TiO₂ photocatalysts were reported. TiO₂ doped with F (Yu et al, 2002), I (Hong et al., 2005) and P (Yu et al., 2003) showed higher photocatalytic activity under UV light and TiO₂ doped with N (Irie et al., 2003a; Asahi et al., 2007), C (Sakthivel and Kisch, 2003), S (Ohno et al., 2003) and codoped with Ni and B (Zhao et al., 2004) showed high photocatalytic activity under visible light. Sato et al.,(2005) have shown efficient photooxidation of CO under visible irradiation by a nitrogen-doped TiO₂. C-doped TiO₂ was obtained by acid-catalyzed sol-gel process (Lettmann et al., 2001) or by the oxidative annealing of TiC (Irie et al.,2003b). Examples of doping methods and selected properties of non-metal doped-TiO₂ are given in Table 1.

Non-metal doping opens up a new possibility for the development of solar- or day-light-induced photocatalytic materials. In the present work, several own nonmetal-doped photocatalysts are presented: C-doped, B,C codoped and S,N,C- tridoped TiO₂. The selected properties of the obtained photocatalysts were correlated with their photoactivity under visible light. Their intrinsic characteristics were investigated using X-ray diffraction (XRD), X-ray photoelectron spectroscopy (XPS) and UV-Vis spectroscopy. The photocatalytic activity of doped TiO₂ was evaluated by the degradation rate of phenol.

METHODS

PREPARATION OF NONMETAL-DOPED TiO₂ PHOTOCATALYSTS

C-doped TiO₂ was prepared by titanium(IV) isopropoxide (TIP, 97%, Sigma-Aldrich Co.) hydrolysis, followed by precipitate separation, drying at 80°C for 24 h and calcinations at 350°C for 1 h. Low calcination temperature favors to keep residual carbon in photocatalyst structure. Carbon comes from alkoxide TiO₂ precursor. B, C-codoped TiO₂ was obtained by sol-gel method (H-labeled) and by grinding anatase with boron precursors (G-labeled). Boric acid triethyl ester (99%) and boric acid (99%) from Sigma-Aldrich Co) were used as a boron source in both procedures. In sol-gel method, TIP was hydrolyzed in the presence of appropriate dopant, followed by precipitate separation, drying at 80°C for 24 h and calcinations at 450°C for 1 h. Titanium dioxide ST-01 from Ishihara-Sangyo, Japan, was used in the second proce-

ture. ST-01 has 320 m²/g specific surface area and consists only of crystalline anatase phase with 7 nm particle size. Boron-modified TiO₂ powders were prepared by grinding ST-01 in agate mortar with H₃BO₃ or (C₂H₅O)₃B, respectively. The obtained powders were dried for 24h at temperature 80°C and calcinated at 450°C.

S, N, C-tridoped photocatalysts were obtained by sol-gel method. Thioacetamide (99%) from POCH S.A. and thiourea (99%) from Sigma-Aldrich Co. were used as sulfur and nitrogen source in catalyst preparation procedures. TIP was hydrolyzed in the presence of appropriate dopant, followed by precipitate separation, drying at 80°C for 24 h and calcinations at 450°C for 1 h. The detailed experimental procedure can be found in previous studies (Zaleska et al., 2007; Zaleska et al., 2008; Górska et al., 2008).

CHARACTERIZATION

ESCALAB-210 spectrometer (VG Scientific) was used for X-ray photoelectron spectroscopy (XPS) measurements with the Al K α X-ray source operated at 300W (15kV, 20mA). The spectrometer chamber pressure was about 5 \times 10⁻⁹mbar. The survey spectra were recorded for all the samples in the energy range from 0 to 1350 eV with 0.4 eV step. High resolution spectra were recorded with 0.1 eV step, 100 ms dwell time and 20 eV pass energy. 90° take-off angle was used in all measurements. AVANTAGE data system software served for curve fitting. The background was fit using nonlinear Shirley model. Scofield sensitivity factors and measured transmission function were used for quantification. Carbon contamination C1s peak at 284.60 eV was used as reference of binding energy. The catalyst powder crystal structure was determined from XRD pattern measured in the range of 2 θ =20÷80° using X-ray diffractometer (Xpert PRO-MPD, Philips) with Cu target K α -ray (λ =1.5404 Å). The diffuse absorption spectra DRS were characterized using UV-VIS spectrometer (Jasco, V-530) equipped with an integrating sphere accessory for diffuse reflectance.

ASAP 2405 instrument (Micromeritics) was used for measurements of BET surface area and pore size of the catalysts by physical adsorption and desorption of nitrogen. The S_{BET} values were calculated according to the BET method using adsorption data at relative pressures p/p_0 between 0.05 and 0.25, where p and p_0 denote the equilibrium pressure. Mesopore-size distribution was calculated with the Barrett-Joyner-Halenda method of isotherm.

MEASUREMENT OF PHOTOCATALYTIC ACTIVITY

The photocatalytic activity of doped-TiO₂ powders in visible light ($\lambda > 400$ nm) was estimated by measuring the decomposition rate of phenol (0.21 mmol/dm³) in an aqueous solution. Photocatalytic degradation runs were proceeded with blind tests in the absence of catalyst or illumination.

25 cm³ of catalyst suspension (125 mg) was stirred using magnetic stirrer and aerated (5 dm³/h) prior and during the photocatalytic process. Aliquots of 1.0 cm³ of the aqueous suspension were collected at regular time periods during irradiation and filtered through syringe filters (Ø=0.2 µm) to remove catalyst particles. Phenol concentration was estimated by colorimetric method using UV-VIS spectrophotometer (DU-7, Beckman). The suspension was irradiated using 1000 W Xenon lamp (Oriol), which emits both UV and Vis light. To limit the irradiation wavelength, the light beam was passed through GG400 to cut-off wavelengths shorter than 400 nm.

RESULTS AND DISCUSSION

The selected properties of nonmetal-doped photocatalysts and pure TiO₂ as a reference sample are given in Table 2. Phenol degradation rate was calculated as an average phenol amount removal after 60 min. visible light illumination. It was observed, that C-doped TiO₂ (sample T_350 obtained by TIP hydrolysis without any dopant and calcination at 350°C) revealed similar photoactivity to S,N,C-tridoped TiO₂ (sample TH_5 obtained by modification with thiourea). Phenol degradation rate under visible light was 2.93 and 2.82 µmol·dm⁻³·min⁻¹ for TH_5 and T_350, respectively. For pure TiO₂ the observed phenol degradation ranged from 0.6 (TiO₂ prepared by sol-gel method) to 0.9 µmol·dm⁻³·min⁻¹ (commercially available TiO₂ ST01).

The obtained results suggested that visible-light-activated TiO₂ could be prepared by carbon, sulfur, nitrogen or boron doping or co-doping of those moieties. For TiO₂ modified with thioacetamide, thiourea or boric acid triethyl ester, phenol degradation rate exceeded 2 µmol·dm⁻³·min⁻¹.

XRD was used to investigate the phase structure of nonmetal-doped TiO₂ powders (see data on crystalline phase in Table 2). For all highly-active C-doped and S,N,C-tridoped photocatalysts a homogenous crystalline phase of anatase appeared in the XRD pattern. B,C-codoped TiO₂ obtained by the sol-gel method, except the sample BA-H(0.5), appeared as amorphous TiO₂, while pure TiO₂ obtained by the same method without any dopant was in the anatase form. Addition of (C₂H₅O)₃B or H₃BO₃ inhibited crystallite growth and/or transformation from amorphous to anatase structure. Only addition of the smallest amount of H₃BO₃ (0.5 wt.%), resulted in anatase structure (Table 2).

All samples obtained by grinding of ST-01 with boron compounds still contained the anatase phase. The XRD pattern of samples BA-G(10) and BE-G(10) shows diffraction lines attributed to the diboron trioxide phase besides the peak due to anatase. Chen et al.,(2006) found that appearance of separate boron phase is related not only to the calcination temperature but also the molar ratio of B to Ti. For samples with molar ratio Ti : B =10 the diboron trioxide crystal appeared during calcination over 600°C. When Ti : B was 20, the B₂O₃ phase emerged at 500°C. In our study, B₂O₃ structure

was observed for samples prepared by grinding with 10 wt.% of boron in two different precursors. Apparently 0.5 wt.% was not enough to form clearly evident B_2O_3 .

Table 2. Visible-light activity of nonmetal-doped TiO_2 photocatalysts

Doping moiety	Sample name*	Dopant precursor**	Dopant amount [wt. %]	Calcination temperature [°C]	Phase composition	Band gap energy [eV]	Phenol decomposition reaction rate [$\mu\text{mol}\cdot\text{dm}^{-3}\cdot\text{min}^{-1}$]
S, N, C	TA0.5	thioacetamide	0.5	450	anatase	3.37	1.8
	TA1	thioacetamide	1.0	450	anatase	3.36	2.1
	TA2	thioacetamide	2.0	450	anatase	3.36	2.3
	TA5	thioacetamide	5.0	450	anatase	3.36	2.4
	TH0.5	thiourea	0.5	450	anatase	3.34	1.3
	TH1	thiourea	1.0	450	anatase	3.33	1.2
	TH2	thiourea de	2.0	450	anatase	3.37	2.5
	TH5	thiourea	5.0	450	anatase	3.37	2.9
B, C	BE-H(0.5)	BATE	0.5	450	amorphous	3.28	0.5
	BE-H1	BATE	1.0	450	amorphous	3.37	0.7
	BE-H(5)	BATE	5.0	450	amorphous	3.41	0.5
	BE-H(10)	BATE	10.0	450	amorphous	3.36	0.8
	BE-G(0.5)	BATE	0.5	450	anatase	3.36	2.1
	BE-G(10)	BATE	10.0	450	anatase + B_2O_3	3.37	1.4
	BA-H(0.5)	boric acid	0.5	450	anatase	3.34	0.6
	BA-H(10)	boric acid	10.0	450	amorphous	3.40	0.9
	BA-G(0.5)	boric acid	0.5	450	anatase	3.30	0.6
	BA-G(10)	boric acid	10.0	450	anatase + B_2O_3	3.33	0.7
C	T_350	no dopant	-	350	anatase	3.41	2.8
-	T_450	no dopant	-	450	anatase	3.33	0.6
	TiO_2 ST-01	no dopant	-	450	anatase	3.30	0.9

* TA, TH, BE-H and BA-H series – prepared by TIP hydrolysis in the presence of an appropriate dopant; BE-G and BA-G series – prepared by grinding of ST01 with an appropriate dopant

** BATE - boric acid triethyl ester

The band gap for doped- TiO_2 fluctuated from 3.28 to 3.41 eV. The highest E_g was observed for highly active C-doped TiO_2 (sample T_350 obtained by TIP hydrolysis followed by calcination at 350°) and inactive B,C-codoped TiO_2 (sample BE-H(5) prepared by sol-gel method using 5 wt.% of boric acid triethyl ester), see Table 2. Band gap narrowing has not been observed in case of any nonmetal-doped TiO_2 , which is in good agreement with theoretical calculation made by Xu et al.,(2006), but contrary to Asahi et al.,(2001) hypothesis. Asahi et al.,(2001) postulated band gap narrowing as the main modification mechanism of TiO_2 doped with nonmetals.

Usually, nonmetal doping affects light absorption characteristics of TiO₂. Figure 1 shows the UV-vis diffuse reflectance spectra of pure TiO₂, S,N,C-tridoped TiO₂ (Fig. 1A) and B,C-codoped TiO₂ (Fig. 1B). All nonmetal-doped TiO₂ powders better absorbed visible light, however, the red shift is negligible. Photoabsorption in the visible region was stronger for TiO₂ doped with S, N, B or C atoms than for pure TiO₂ (Fig. 1). Only for S,N,C-tridoped TiO₂ clear correlation between absorption spectra and photoactivity was observed, i.e. for increased photoactivity absorption in visible region also increased (reflectance decreased).

To investigate the chemical states of nonmetals atoms incorporated into TiO₂ binding energies were measured by X-ray photoemission spectroscopy. Table 3 shows chemical content, as well as phenol degradation efficiency under visible light, for selected – the most active photocatalysts. Photocatalysts are listed from higher to lower photoactivity. In all doped-TiO₂ samples the peak attributed to C 1s at around 289-284 eV was observed. In most cases, the C 1s region consists of three peaks: the first peak (~288.9 eV) related to COOH groups bonds, the second peak (~286 eV) to C-OH bonds and the third peak (~284.6 eV) related to C-C aromatic bonds. Thus, carbon content is presented as a total C content, C-C structure (both C-C_{alif} and C-C_{arom}) and as carbon in form of C-C_{arom}. All visible-light-activated photocatalysts contain carbon including carbon in the form of C-C_{arom}.

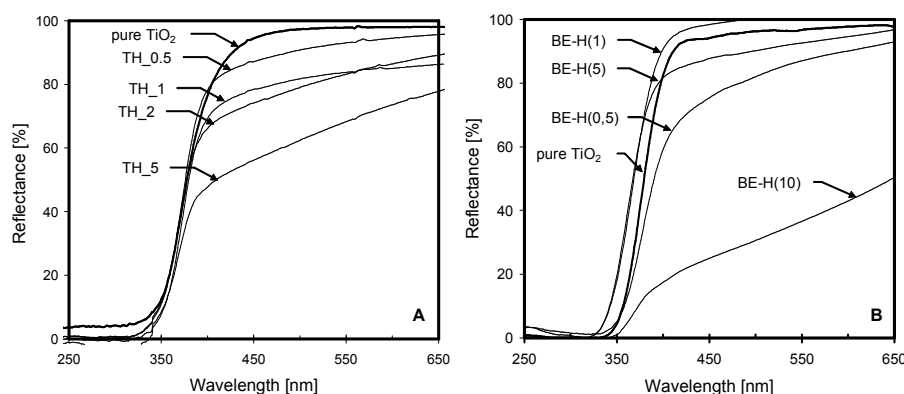


Fig. 1. Diffuse reflectance spectra of pure and doped-TiO₂: (A) S,N,C-tridoped TiO₂ prepared by hydrolysis of TIP in the presence of thiourea, (B) B,C-codoped TiO₂ prepared by hydrolysis of TIP in the presence of (C₂H₅O)₃B

Among all obtained powders, the highest visible-light activity was observed for the S,N,C-tridoped TiO₂ - prepared with 5 wt.% of thiourea. The rate constant for phenol and 4-chlorophenol decomposition was 0.054 and 0.041 min⁻¹, respectively. The most effective catalyst contained 1.3 at.% of nitrogen, 7.21 at.% of carbon and 0.33 at. % of sulfur, as indicated by XPS analysis. TH5 sample is one of the richest in sulfur (Table 3), mainly in S⁶⁺ species. On the other hand, TH5 carbon content remained in medium range.

Table 3. Chemical characterization of most visible light activated TiO₂ photocatalysts

Sample No	XPS-determined content, [at.%]						Phenol degradation efficiency after 60 min. irradiation
	ΣC	C-C	C-C _{arom}	S	N	B	
TH_5	7.21	3.69	1.71	0.33	1.3	-	97
T_350	15.2	10.1	10.1	-	-	-	82
TH_2	14.89	9.86	9.86	0.33	1.15	-	82
TA_5	6.37	4.95	2.76	0.16	1.24	-	81
TA_2	2.52	1.5	0.83	-	1.21	-	72
BE-G(0.5)	18.54	12.77	12.77	-	-	3.21	61
BE-G(10)	18.43	9.55	9.55	-	-	12.33	45

High visible-light activity was also observed for C-doped TiO₂, containing residual carbon from organic titanium dioxide precursor. Since surface area and pore size distribution are important factors for heterogeneous photocatalysis, the sample T_350 had high BET surface area (205.8 m²/g) and small crystallite size (8.4 nm) and average pore diameter (8.3 nm). Enhanced visible light-activity probably results from the presence of carbon (15.2 at.%), mainly in the form of C-C species, as well as from high surface area. Although, there is no red shift observed for sample T_350, it exhibited better light absorption in Vis – moreover, the absorption tail was extended to 750 nm.

According to Sakthivel and Kisch (2001) hypothesis, there is an optimal amount of dopant responsible for enhanced visible light activity. Besides the dopant amount, the chemical character of incorporated element is also important. Literature data and obtained results suggested that carbon in the form of carbonate and boron as boron trioxide suppress visible-light activity. Lettmann et al.,(2001), as well as Umabayashi et al.,(2003) stated that carbon species works as sensitizer and single oxygen is formed without TiO₂ excitation. Yu and co-workers (2005) provided an alternative explanation that sulfur doping can indeed create intra-band gap states close to the conduction band edges, and thus induces visible-light absorption at the sub-band energy. It was also found, that constitution of the TiO₂ (doped and undoped TiO₂) also plays an important role in its high photoactivity (Yu et al., 2006). Usually, the composite of two kinds of semiconductor or two phases of the same semiconductor is beneficial in reducing the recombination of photo-generated electrons and holes, and thus enhances photocatalytic activity. The interface between the two phases may act as a rapid separation site for the photo-generated electrons and holes due to the difference in the energy level of their conduction bands and valence bands. Therefore, Yu et al.,(2006) suggested that N,S-codoped TiO₂ powders prepared by hydrolysis method exhibit significant photoactivity under daylight illumination due to the fact that the as-prepared TiO₂ powders consist of two phases of undoped TiO₂ and N,S-codoped TiO₂.

CONCLUSION

1. Using several new dopants, a series of TiO₂ catalyst samples was selected for investigation aimed at correlation of their structure and photoactivity. Particularly S,N,C-tridoped (obtained by TIP hydrolysis in the presence of thioacetamide and thermal treating at 450°C) and C-doped (obtained by TIP hydrolysis in the absence of any dopant and thermal treating at 350°C) photocatalysts were active under visible light at wavelengths greater than 400 nm.
2. B³⁺, S⁺ and carbon in the form of C-C_{arom.} species showed beneficial influence on photodegradation efficiency in visible light.
3. For S,N,C-tridoped photocatalysts, the experimental data clearly indicate the presence of correlation between absorption and photoactivity of the obtained powders - for increased photoactivity absorption in visible region also increased.
4. The experimental data confirm earlier observations, that a lack of band gap narrowing with simultaneous increase of the absorption intensity can still lead to effective degradation of the organic compounds, which is mainly controlled by presence of sensitizers (residual carbon).

ACKNOWLEDGMENTS

This research was supported by Polish Ministry of Science and Higher Education (contract No.: N205 077 31/3729). Dr. Beata Tryba from Department of Water Technology and Environmental Engineering, Szczecin University of Technology is gratefully acknowledged for assistance in UV-Vis spectroscopy.

REFERENCES

- ANPO M., (2000) Use of visible light. Second-generation titanium dioxide photocatalysts prepared by the application of an advanced metal ion-implantation method. *Pure Appl. Chem.* 72, 1787-1792.
- ASAHI, R., MORIKAWA, T., (2007) Nitrogen complex species and its chemical nature in TiO₂ for visible-light sensitized photocatalysis. *Chem. Phys.* 339, 57-63.
- ASAHI, R., MORIKAWA, T., OHWAKI, T., AOKI, K., TAGA, Y., (2001) Visible-Light Photocatalysis in Nitrogen-Doped Titanium. *Science* 293, 269-271.
- CHEN, C., BAI, H., CHANG, S., CHANG, C., DEN, W., (2007) Preparation of N-doped TiO₂ photocatalyst by atmospheric pressure plasma process for VOCs decomposition under UV and visible light sources. *J. Nanoparticle Res.* 9, 365-375.
- CHEN, D., YANG, D., WANG, Q., JIANG, Z., (2006) Effects of boron doping on photocatalytic activity and microstructure of titanium dioxide nanoparticles. *Ind. Eng. Chem. Res.* 45, 4110-4116.
- FUJISHIMA, A., ZHANG, X., (2006) Titanium dioxide photocatalysis: present situation and future approaches. *C.R. Chimie* 9, 750-760.

- GÓRSKA, P., ZALESKA, A., KLIMCZUK, T., SOBCZAK, J.W., SKWAREK, E., HUPKA, J., (2008) The influence of calcinations temperature on TiO₂ structure, surface properties and photoactivity under UV and visible light. *Appl. Catal.* doi: 10.1016/j.apcatb.2008.04.028.
- HONG, X.T., WANG, Z.P., CAI, W.M., LU, F., ZHANG, J., YANG, Y.Z., MA, N., LIU, Y.J., (2005) Visible-Light-Activated Nanoparticle Photocatalyst of Iodine-Doped Titanium Dioxide. *Chem. Mater.* 17, 1548-1552.
- IRIE, H., WATANABE, Y., HASHIMOTO, K., (2003) Carbon-doped anatase TiO₂ powders as a visible-light sensitive photocatalyst. *Chem. Lett.* 32, 772-773.
- IRIE, H., WATANABE, Y., HASHIMOTO, K., (2003) Nitrogen-concentration dependence on photocatalytic activity of TiO₂-xNx powders. *J Phys Chem B* 107, 5483-5486.
- LETTMANN, C., HILDEBRAND, K., KISCH, H., MACYK, W., MAIER, W.F., (2001) Visible light photodegradation of 4-chlorophenol with a coke-containing titanium dioxide photocatalyst. *Appl. Catal. B* 32, 215-227.
- MOON, S.C., MAMETSUKA, H., TABATA, S., SUZUKI, E., (2007) Photocatalytic production of hydrogen from water using TiO₂ and B/TiO. *Catal. Today* 58, 125-132.
- OHNO, T., AKIYOSHI, M., UMEBAYASHI, T., ASAI, K., MITSUI, T., MATSUMURA, M., (2004) Preparation of S-doped TiO₂ photocatalysts and their photocatalytic activities under visible light. *Appl. Catal. A* 265, 115-121.
- OHNO, T., MITSUI, T., MATSUMURA, M., (2003) Photocatalytic activity of S-doped TiO₂ photocatalyst under visible light. *Chem. Lett.* 32, 364-365.
- SAKTHIVEL, S., KISCH, H., (2003) Daylight photocatalysts by carbon-modified titanium dioxide. *Angew Chem Int Ed* 42, 4908-4911.
- SATO, S., NAKAMURA, R., ABE, S., (2005) Visible Light sensitization of TiO₂ photocatalysts by wet-method N doping. *Appl. Catal. A* 284, 131-137.
- TAKEUCHI, K., NAKAMURA, I., MATSUMOTO, O., SUGIHARA, S., ANDO, M., IHARA, T., (2000) Preparation of visible-light-responsive titanium oxide photocatalysts by plasma treatment. *Chem. Lett.* 29, 1354-1355.
- UMEBAYASHI, T., YAMAKI, T., TANAKA, S., ASAI, K., (2003) Visible Light-Induced Degradation of Methylene Blue on S-doped TiO₂. *Chem. Lett.* 32, 330-331.
- XU, T., SONG, C., LIU, Y., HAN, G., (2006) Band structures of TiO₂ doped with N, C and B. *Zhejiang Univ Science B* 7, 299-303.
- YU, J., ZHOU, M., CHENG, B., ZHAO, X., (2006) Preparation, characterization and photocatalytic activity of in situ N,S-codoped TiO₂ powders. *J. Molec. Catal. A* 246, 176-184.
- YU, J.C., HO, W., YO, J., YIP, H., WONG, P.K., ZHAO, J., (2005) Efficient visible-light-induced photocatalytic disinfection on sulfur-doped nanocrystalline titania. *Environ. Sci. Technol.* 39, 1175-1179.
- YU, J.C., YU, J., HO, W., JIANG, Z., ZHANG, L., (2002) Effects of F- Doping on the Photocatalytic Activity and Microstructures of Nanocrystalline TiO₂ Powders. *Chem. Matter.* 14, 3808-3816.
- YU, J.C., ZHANG, L., ZHENG, Z., ZHAO, J., (2003) Synthesis and Characterization of Phosphated Mesoporous Titanium Dioxide with High Photocatalytic Activity. *Chem. Matter.* 15, 2280-2286.
- ZALESKA, A., GÓRSKA, P., SOBCZAK, J.W., HUPKA, J., (2007) Thioacetamide and thiourea impact on visible light activity of TiO₂. *Appl. Catal. B* 76, 1-8.
- ZALESKA, A., SOBCZAK, J.W., GRABOWSKA, E., HUPKA, J., (2008) Preparation and photocatalytic activity of boron-modified TiO₂ under UV and visible light. *Appl. Catal. B* 78, 92-100.
- ZHAO, W., MA, W., CHEN, C., ZHAO, J., SHUAI, Z., (2004) Efficient degradation of toxic pollutants with Ni₂O₃/TiO₂-xBx under visible irradiation. *A. Am. Chem. Soc.* 126, 4782-4783.

Zaleska A., *Characteristics of doped-TiO₂ photocatalysts*, Physicochemical Problems of Mineral Processing, 42 (2008), 213-224 (w jęz. ang)

Fotokatalityczne właściwości TiO₂ wykorzystywane są między innymi do eliminacji substancji organicznych z fazy gazowej i ciekłej oraz w samooczyszczaniu powierzchni. Tlenek tytanu (IV) absorbuje prawie wyłącznie promieniowanie UV, dlatego podczas fotokatalizy wykorzystać można zaledwie od 3 do 5 % promieniowania słonecznego. Zatem otrzymanie półprzewodnika tytanowego nowej generacji aktywnego w zakresie promieniowania widzialnego ($\lambda > 400$ nm), znacząco rozszerzyłoby możliwości aplikacyjne fotokatalizy heterogenicznej w ochronie środowiska, przez wykorzystanie głównej części spektrum światła słonecznego lub zastosowanie źródła światła o mniejszym natężeniu promieniowania. W niniejszej pracy omówiono nowe fotokatalizatory aktywne pod wpływem światła widzialnego, otrzymane poprzez modyfikację TiO₂ związkami siarki, azotu, boru oraz węgla. Fotoaktywność otrzymanych fotokatalizatorów została odniesiona do charakteru chemicznego wprowadzonej domieszki, struktury krystalicznej, wielkości krystalitów, powierzchni właściwej fotokatalizatora oraz metody otrzymywania.

słowa kluczowe: półprzewodnik-TiO₂, fotokataliza heterogeniczna, fotokatalizatory aktywne pod wpływem światła widzialnego